DOI: 10.1002/asia.200800322

Imidazole-Annulated Tetrathiafulvalenes Exhibiting pH-Tuneable Intramolecular Charge Transfer and Redox Properties

Jincai Wu,[a,b] Nathalie Dupont,[c] Shi-Xia Liu,*[a] Antonia Neels,[d] Andreas Hauser,[c] and Silvio Decurtins[a]

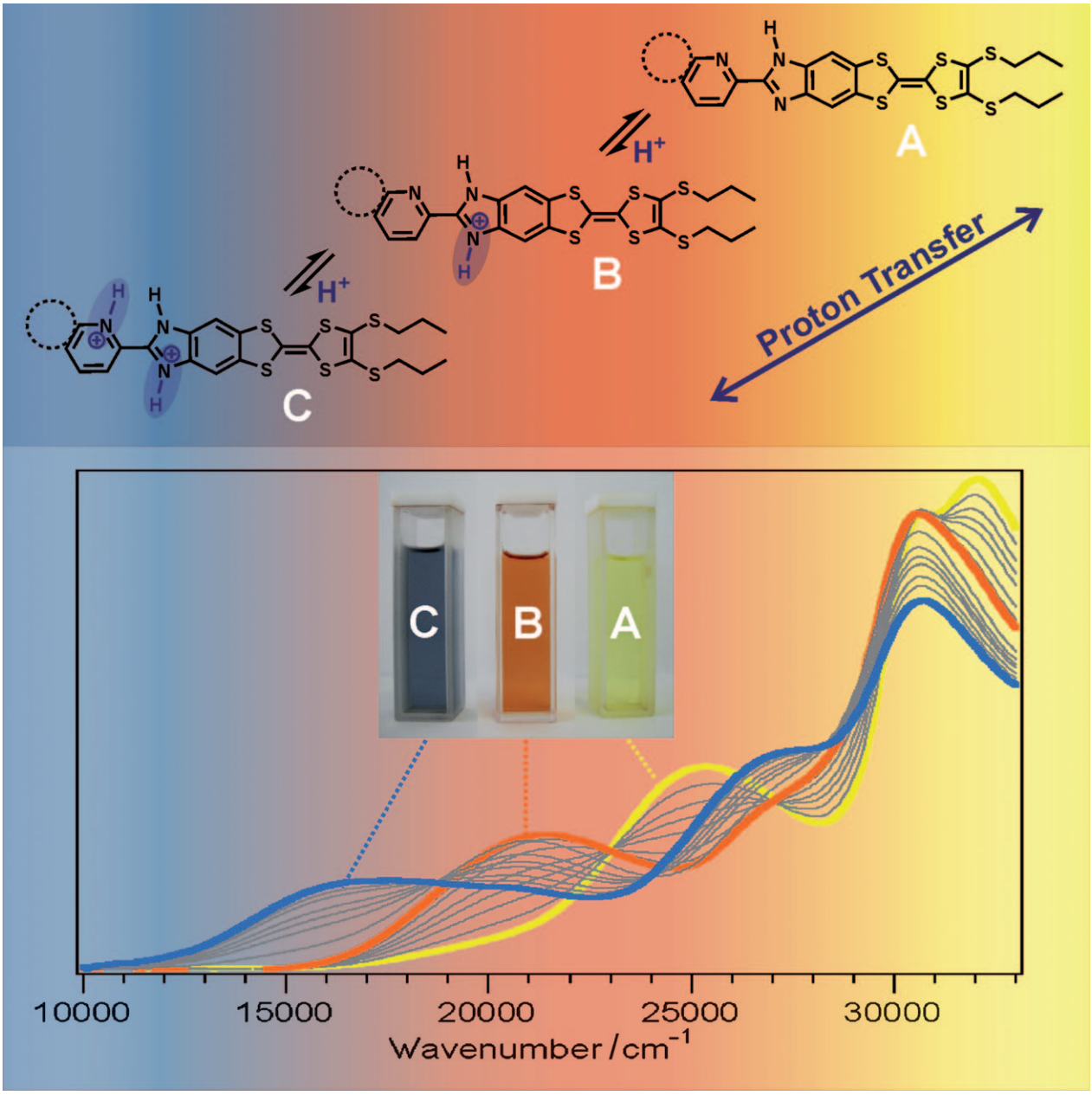

Abstract: In order to study the electronic interactions in donor–acceptor ensembles as a function of pH, an efficient synthetic route to three imidazole-annulated tetrathiafulvalene (TTF) derivatives **1**–**3** is reported. Their electronic absorption spectra, in view of photoinduced intramolecular charge transfer, and their electrochemical behavior were investigated, and pK_a values for the two protonation processes on the acceptor unit were determined in organic solvents by photometric titration. The influence of the TTF moiety on these values is discussed.

Keywords: charge transfer · donor-acceptor systems · sensors · tetrathiafulvalene · UV/Vis spectroscopy

Introduction

Electrochemically amphoteric compounds are of current interest owing to their potential applications in molecular electronics and optoelectronics, whereby organic compounds possessing a high degree of conjugation are particularly interesting for advanced electronic applications.[1] Accordingly, efforts have been directed to the design and synthesis of molecular systems composed of building blocks that give rise to electron donor (D) and acceptor (A) interactions. Amongst all kinds of molecular electron donor moieties, tetrathiafulvalene (TTF) and its derivatives are known to be strong π-donors capable of forming persistent cation radical and dication species upon oxidation, thus leading to a number of conducting and superconducting materials.[2] In this context, the effective intermolecular orbital overlap in π-stacked assemblies is highly sensitive to chemical modifications of the TTF framework and this plays a crucial role in the electronic conductivity. Thus, in order to achieve a highly ordered molecular organization in charge-transfer (CT) salts, the self-assembling ability and the dimensionality of the electronic structure has been enhanced primarily by chalcogen–chalcogen interactions[2] and halogen or hydrogen bonds.[3–5] Notably, amongst them, TTF–imidazole systems exhibit unprecedented electronic and structural modulation effects of hydrogen bonds giving rise to a number of highly conductive CT complexes with various acceptors.[5]

With respect to covalently linked D–A ensembles, important variables, besides the nature of the donor and acceptor components, are their relative distance, orientation, and the degree of electronic coupling between them. Normally, the D and A components are held together by π-spacers such as oligo(phenylene ethynylene), oligo(phenylene vinylene), oligothiophene, or σ-spacers of variable length and flexibility.[6] Alternatively, only a few examples of annulated TTF–π-acceptor systems have been reported in the literature so far, for example, TTF-diquinones.[7] For a current overview of D–A ensembles the reader may consult the recent review by Wudl et al.[8]

Along this line, we recently introduced a synthetic concept for the annulation of TTF derivatives to a variety of acceptor moieties and reported synthetic routes to intimately fused and rigid D−π−A ensembles, as exemplified by compounds with i) four TTF moieties fused to phthalocyanine cores;[9] ii) three TTF moieties fused to a hexaazatriphenylene core;[10] iii) one TTF annulated with dipyrido-[3,2-*a*:2′,3′-*c*]phenazine;[11] and iv) one TTF coupled to *N*,*N*′-phenylenebis(salicylideneimine).[12] In all these examples a main principle emerges, namely the molecular D–A systems are tailored into planar configurations exhibiting defined symmetries which provides a defined geometrical control. They are also specifically designed for chelation of various metal ions.[12–13] As a continuation of our ongoing studies, we present here an efficient synthetic route to further organic π-conjugated D–A molecules which contain the TTF unit as a donor and an *N*,*N*-diimine chelating ligand—in form of 2-(2-pyridyl)benzimidazole (PB), 2-(2-quinolinyl)benzimidazole (QB), or its derivative 2-(6-methoxy-2-quinolinyl)benzimidazole (MQB)—as an acceptor (**1**–**3**, Figure 1).

The general interest in imidazole compounds stems from their specific structural features and biological activity,[14] including anti-ulcer, anti-tumour, and anti-viral effects. The heterocyclic aromatic compounds reveal strong and directional hydrogen bond interactions, and act as Brönsted acids and bases. They thus play an important role as a relay for

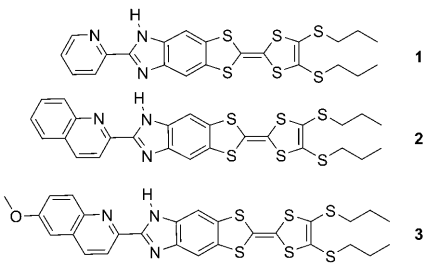

Figure 1. Structures of the D–A molecules **1**–**3**.

[a] Prof. J. Wu, Dr. S.-X. Liu, Prof. S. Decurtins
Departement für Chemie und Biochemie
Universität Bern
Freiestrasse 3, CH-3012 Bern (Switzerland)
Fax: (+41) 31-631-3995
E-mail: liu@iac.unibe.ch

[b] Prof. J. Wu
College of Chemistry and Chemical Engineering
State Key Laboratory of Applied Organic Chemistry
Lanzhou University, 730000 Lanzhou (P.R. China)

[c] N. Dupont, Prof. A. Hauser
Département de chimie physique, Sciences II
Université de Genève
30, Quai Ernest-Ansermet, CH-1211 Genève 4 (Switzerland)

[d] Dr. A. Neels
XRD Application LAB
CSEM Centre Suisse d'Electronique et de Microtechnique SA
Jaquet-Droz 1, Case postale, CH-2002 Neuchâtel (Switzerland)

Supporting information for this article is available on the WWW under http://dx.doi.org/10.1002/asia.200800322.

proton transfer (PT) processes, which are among the most extensively studied chemical processes, owing to their importance in nature.[15] As a consequence, imidazole derivatives have attracted much attention in fields such as crystal engineering,[16] molecule-based magnets,[17] molecular conductors,[18] and fluorescence sensors.[19]

A primary feature of compounds **1**–**3** is that a range of functionalities on the acceptor part is combined in close and controlled proximity with the fused TTF donor part. For the former, the aromatic imidazole, with its pyridine- and pyrrole-like N atoms, introduces an amphoteric character as a moderately strong base and a weak acid, and the linked pyridine or quinoline adds another basic N atom. Moreover, the resulting N^N chelating site makes these molecules attractive ligands for complexation to various metal ions. As a most striking feature, discussed in detail below, the annulated TTF donor shows a photoinduced intramolecular charge-transfer (ICT) transition in its absorption spectrum, which is sensitive to the different protonation states on the acceptor site.

In this article, we describe the synthesis of three TTF-PB/QB/MQB molecules (**1**–**3**) and the single-crystal X-ray structure for **1**. In addition, the results of an electrochemical and a photophysical investigation at various pH values are discussed.

Results and Discussion

As outlined in Scheme 1, the target compounds **1**–**3** were obtained by the direct condensation reaction of the corresponding aldehydes with 5,6-diamino-2-(4,5-bis(propylthio)-1,3-dithio-2-ylidene)-benzo [*d*]-1,3-dithiole in acceptable yields. All compounds were easily purified by flash chromatography on SiO_2 and have been fully characterized by NMR, EI mass spectrometry, and elemental analysis.

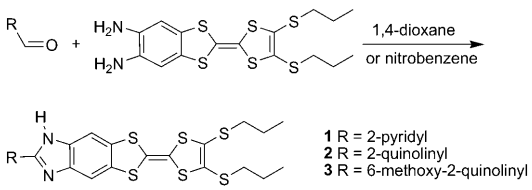

Scheme 1. A synthetic route to D–A molecules **1**–**3**.

Orange needle-shaped single crystals of **1** suitable for X-ray analysis were obtained by slow evaporation of its solution in CH_3CN. The molecule **1** crystallizes in a monoclinic space group (*C*2/*c*) and an ORTEP drawing of the molecule with the atomic numbering scheme is shown in Figure 2. Apparently, this compound adopts a non-planar conformation

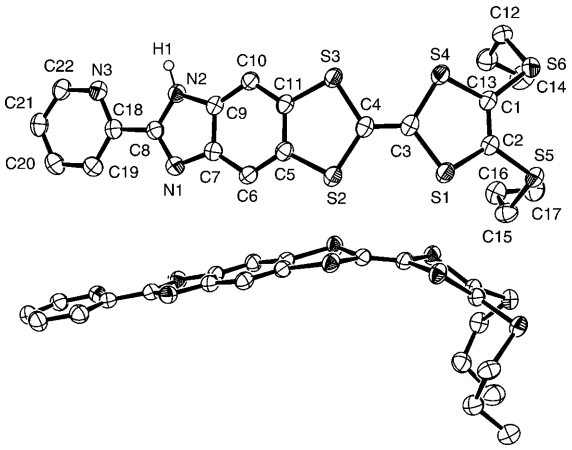

Figure 2. ORTEP drawing and atomic numbering Scheme of the molecule **1** with thermal ellipsoids at 50% probability level. Hydrogen atoms, except for the one on the imidazole ring, have been omitted for clarity. Front and side views are presented.

along its long molecular axis, and specifically the TTF moiety shows a boat conformation, folding along the S1···S4 and S2···S3 vectors by 28.9(1)° and 18.24(1)°, respectively. In contrast to the TTF part, all atoms of the PB unit lie almost perfectly within a plane; the rms deviation from a least-squares plane through all involved atoms of PB is 0.01 Å. Notice, that the nitrogen atoms N1 and N3 are situated in a *trans* orientation within the solid state structure. The bond distances within the TTF and PB moieties are in the expected ranges in comparison with those of similar compounds in the literature.[5c,20–21] Figure 3 highlights the alternating arrangement of the molecules in the crystal structure. A noticeable feature is the head-to-tail alignment caused by π···π stacking between the PB moieties to afford dimers, which are, in addition, linked parallel to each other by N–H···N hydrogen bonds and short S···S contacts.

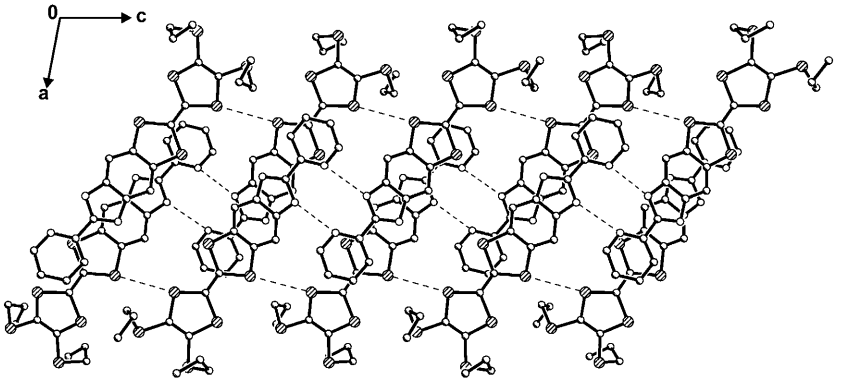

Figure 3. Crystal packing of **1** showing hydrogen bonds (N–H···N, 2.960 Å) and close S···S contacts of 3.536 Å (dashed lines).

The electrochemical properties of the π-conjugates **1–3** were investigated by cyclic voltammetry (CV) in dichloromethane. All of them show two reversible single-electron oxidation waves typical of the TTF system, corresponding to $E_{1/2}^1$ and $E_{1/2}^2$ in Table 1. Obviously, the presence of the different substituents at the 2-position of the imidazole ring has a negligible influence on the electron-donating ability of TTF. Remarkably, with successive addition of HCl to **1–3**, both redox processes of the TTF unit are clearly shifted suggesting the occurrence of two new redox species. Taking **1** as an example (Figure 4),[22] both oxidation potentials are, at

Table 1. Redox Potentials (V vs Ag/AgCl) of **1–3** in CH_2Cl_2.

E	**1**	[**1**·H$^+$]	[**1**·2H$^+$]	**2**	[**2**·H$^+$]	[**2**·2H$^+$]	**3**	[**3**·H$^+$]	[**3**·2H$^+$]
$E_{1/2}^1$	0.54	0.63	0.67	0.53	0.61	0.68	0.52	0.60	0.68
$E_{1/2}^2$	0.94	0.98	0.93	0.95	0.99	0.95	0.94	0.98	0.90

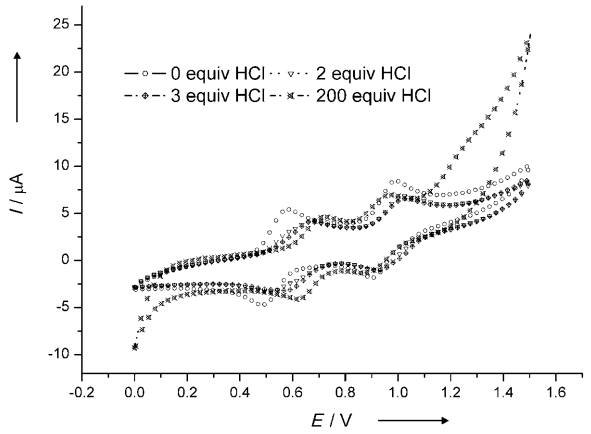

Figure 4. Cyclic voltammogram of compound **1** (10^{-3} M) in the presence of increasing amounts of HCl; CH_2Cl_2; Bu_4NPF_6 (0.1 M); 100 mV s^{-1}; Pt working electrode. V vs Ag/AgCl.

first, substantially positively shifted upon the addition of a small amount of HCl, until, upon the addition of 3 equivalents of HCl, the original $E_{1/2}^1$ wave completely disappears and only two reversible redox waves remain at 0.63 and 0.98 V. The large potential shifts correspond to a decrease in the π-donating ability of the TTF unit arising from the protonation of the imidazole ring in close proximity to the TTF core. Interestingly, a large excess of HCl leads to a further positive shift of $E_{1/2}^1$ but to a negative shift of $E_{1/2}^2$, which is now almost at the same potential as that of the unprotonated **1**.[23] This observation might be attributed to both the occurrence of proton dissociation when the TTF unit undergoes the second oxidation, as shown in the box in Scheme 2, and the significant change in the electrolytic medium caused by the presence of a large excess of HCl. It can therefore be deduced that there is a strongly dynamical difference in the proton dissociation and redox processes, as reported in the literature.[24] All these results indicate the coexistence of three redox species, **1** ($E_{1/2}^1 = 0.54$ V, $E_{1/2}^2 = 0.94$ V) and two protonated ones, that is, [**1**·H$^+$] ($E_{1/2}^1 = 0.63$ V, $E_{1/2}^2 = 0.98$ V) and [**1**·2H$^+$] ($E_{1/2}^1 = 0.67$ V, $E_{1/2}^2 = 0.93$ V), which can be described with the equilibrium processes shown in Scheme 2. It is noteworthy that at particular potentials, constant currents upon addition of HCl are observed, similar to isosbestic points in optical spectroscopy. This is indicative of a concomitant appearance of the corresponding protonated species at the expense of **1**. These observations are in good agreement with the results from UV/Vis spectroscopy measurements. Moreover, as shown with the curve (crossed triangle) in Figure 4, the current increases appreciably around 1.1 V, while it decreases around 0 V. When measurements under identical conditions from −1.7 to 1.7 V were performed, one irreversible anodic peak at 1.2 V and one irreversible broad cathodic peak at −0.3 V appeared. We expect that these irreversible redox processes occur at the pyridine functional group. Such phenomena are also observed in analogous TTF compounds, but have not been discussed in detail.[25]

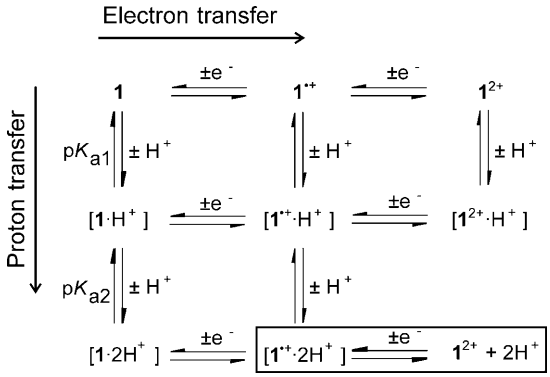

Scheme 2. Equilibrium reactions during the electrochemical titration of **1** with H$^+$.

It must also be mentioned that in the negative direction, there are no redox waves observed with successive addition of HCl within the accessible potential window. These findings match well with the large gap between the oxidation and reduction waves estimated from the energy of the ICT band (Table 2).

Table 2. Maxima of the ICT absorption bands for **1–3** and their protonated forms in CH_2Cl_2.

Compound	Absorption [nm]	Absorption [cm^{-1}]	ε [M^{-1} cm^{-1}]
1	397	25189	14800
[**1**·H$^+$]	468	21368	9800
[**1**·2H$^+$]	593	16863	6400
2	421	23753	15500
[**2**·H$^+$]	564	17730	12000
[**2**·2H$^+$]	691	14472	9600
3	412	24272	20900
[**3**·H$^+$]	544	18382	13000
[**3**·2H$^+$]	655	15267	10600

The absorption spectra of **1–3** dissolved in CH_2Cl_2 are presented in Figure 5. They show two domains of broad and intense absorption bands centered around 24000 and

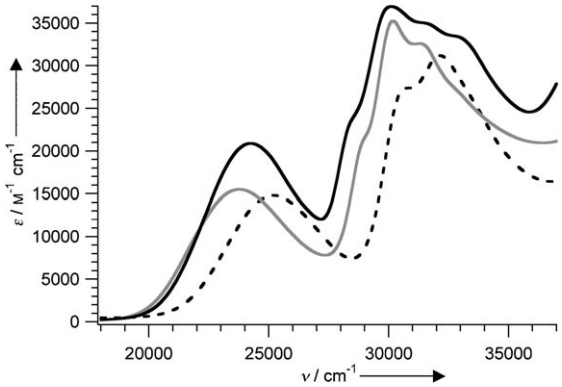

Figure 5. Absorption spectra of **1** (dashed line), **2** (gray line), and **3** (black line) in CH_2Cl_2 at room temperature.

30000 cm^{-1}, respectively. The absorption bands centered at 25189 cm^{-1} (397 nm), 23753 cm^{-1} (421 nm), and 24272 cm^{-1} (412 nm), respectively for **1–3**, result from an ICT transition from the TTF unit to the substituted benzimidazole moieties. In the UV region, strong absorption bands are characteristic for π–π* transitions located on both, the TTF and the substituted benzimidazole subunits.[26]

In order to arrive at a deeper understanding of the fused D–A molecules **1–3**, the protonation characteristics of each compound were experimentally investigated in CH_2Cl_2 solution. The molecules have two protonation sites each, namely, the benzimidazole nitrogen (N1) and the nitrogen on the pyridine (N3) or on the quinoline, respectively. It has already been demonstrated experimentally and theoretically that a benzimidazole nitrogen has a higher proton affinity than that of pyridine.[27] It was on this basis that UV/Vis titration experiments were carried out in order to determine the specific pK_a values of molecules **1–3**.

The UV/Vis spectra of **1** dissolved in CH_2Cl_2, taken as a function of pH, that is, with successive addition of HCl equivalents, are depicted in Figure 6. From 0 to 3 equivalents of HCl, for an initial concentration of 10^{-5} M of **1**, the broad absorption band at 25189 cm^{-1} gradually disappears and a new absorption band at 21368 cm^{-1} emerges. From 3 to 300 equivalents, this new band decreases in intensity and a third absorption band concomitantly appears at 16863 cm^{-1}. A remarkable feature is the occurrence of two quite well defined isosbestic points, at 23000 cm^{-1} for up to 3 equivalents added, and at approximately 18400 cm^{-1} above 3 equivalents. This indicates the presence of three species in two comparatively well separated chemical equilibria, namely compound **1** and the two protonated species [**1**·H^+] and [**1**·2H^+] as shown in Scheme 2. Compounds **2** and **3** show very similar behavior. The corresponding full spectra are given in Figures S3 and S4 of the Supporting Information, the absorption maxima of the species in the neutral and protonated forms are reported in Table 2.

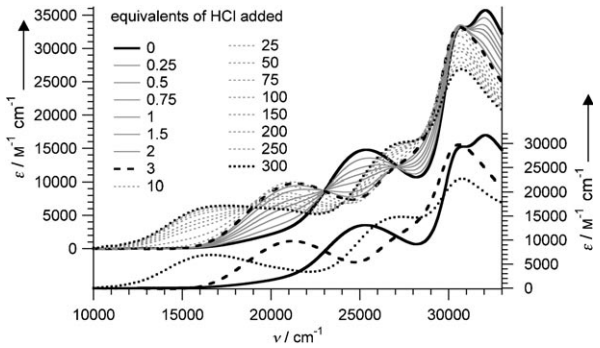

Figure 6. Absorption spectra (top) of **1** in CH_2Cl_2 at room temperature as a function of molar equivalents of HCl added in comparison with the simulation spectra (bottom) at a total concentration of **1** of 10^{-5} M.

In accordance with the absorption spectra, the color of the solution changes reversibly between yellow, orange, and blue during the acid/base titration. Apparently, protonation of the two nitrogen atoms of the PB unit reduces the electron density on the aromatic ring system successively, thereby lowering the energy of the LUMO and increasing its acceptor properties. As a result, the corresponding spectroscopic TTF→PB ICT transition moves to lower energies in two distinct steps of approximately 4000 and 4500 cm^{-1}, respectively. The first step corresponds to the protonation of the imidazole nitrogen, the second step to the protonation of the pyridine nitrogen.

The spectra in Figure 6 can be analyzed quantitatively according to the acid–base equilibria shown in Scheme 2. A factor analysis and single value decomposition[28] on the experimental data supports the assumption of three species in chemical equilibrium, and a least squares fit using the program SPECFIT 3[29] results in the pK_a values for the two protonation steps given in Table 3. The resulting individual

Table 3. Experimental pK_a values for **1–3** and the reference compound 2-(2-pyridyl)benzimidazole (**PB**) in CH_2Cl_2.

pK_a	**PB**	**1**	**2**	**3**
pK_{a1}	4.5(1)	5.5(1)	5.2(1)	4.9(1)
pK_{a2}	3.2(1)	3.1(1)	3.4(1)	3.6(1)

spectra of the three species are included in Figure 6. Figures 7a and b show the experimental evolution of the concentration of the three species as a function of HCl added to the solution for the two protonation steps, as well as the resulting best fit from the single value decomposition. The spectra of compounds **2** and **3** were treated in the same way, the corresponding pK_a values are likewise given in Table 3 and the results of the single value decomposition are shown in Figures S5 and S6 of the Supporting Information.

In the literature, experimental pK_a values in non-aqueous solvents are quite rare. In aqueous solutions, the values of pK_{a1} and pK_{a2} for the reference compound **PB** are given as 4.41 and −1.59, respectively.[27b] In order to compare the values of the TTF annulated compounds in CH_2Cl_2 with the

CHEMISTRY
AN ASIAN JOURNAL

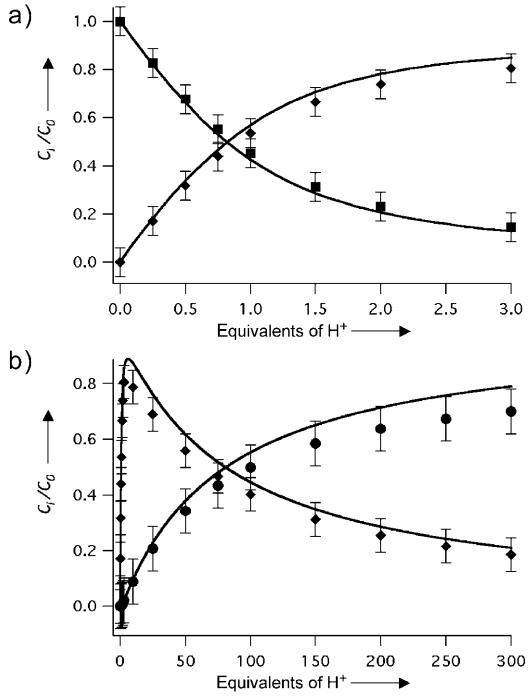

Figure 7. Experimental (symbols) and calculated (full lines) titration curves. For the calculated curves the pK_a values of Table 3 were used: a) first step, **1** (■) and [**1**·H^+] (◆), b) second step [**1**·H^+] (◆) and [**1**·$2H^+$] (●) in CH_2Cl_2 at room temperature and a total concentration of **1** of 10^{-5} M.

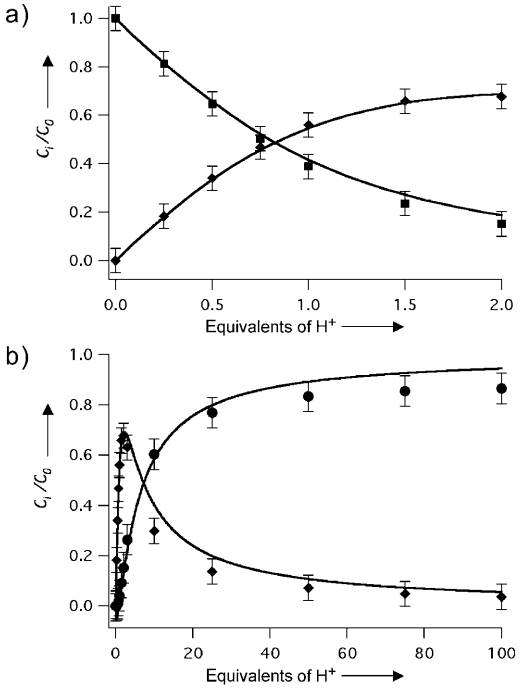

Figure 8. Experimental (symbols) and calculated (full lines) titration curves. For the calculated curves the pK_a values of Table 3 were used: a) first step, **PB** (■) and [**PB**·H^+] (◆), b) second step [**PB**·H^+] (◆) and [**PB**·$2H^+$] (●) in CH_2Cl_2 at room temperature and of total concentration of **PB** of 10^{-4} M.

ones for the compounds without TTF, titration curves were also determined for **PB** in CH_2Cl_2. Figure 8 shows the experimental curves for an initial **PB** concentration of 10^{-4} M together with the best fit from the single value decomposition of the optical spectra (see Figure S7 in the Supporting Information) recorded as a function of equivalents of HCl added. The corresponding pK_a values are included in Table 3. Whereas pK_{a1} has a value close to the one found in aqueous solution, the pK_{a2} value of 3.2 shows that the proton on pyridine is much less acidic in CH_2Cl_2 than in aqueous solution.

In comparison to **PB**, compounds **1–3** show no significant increase in pK_{a2}, that is, for the protonation of N3 (pyridine). In contrast, they show an increase of one unit for pK_{a1}, that is, for the protonation of N1 (benzimidazole). Qualitatively this can be understood as arising from the electron donating properties of the TTF unit, which results in a higher electron density on the PB unit as compared to the compound without TTF, and therefore the pK_{a1} values increase substantially. As expected this effect is restricted to N1, that is, the nitrogen atom on the ring system directly fused to the TTF unit.

Conclusions

In conclusion, three imidazole-annulated TTF derivatives **1–3** have been prepared and fully characterized, and the influence of the TTF unit on the pK_a values of the acceptor units as determined by photometric titration has been discussed. The novel feature of these D–A molecules is that they contain a PB ancillary functionality, which has been incorporated with the following specific roles in mind: i) The presence of three nitrogen atoms as proton donor/acceptors renders them promising in the field of chemosensors. ii) Direct annulation of PB to the TTF core is expected to enhance cooperativity between CT on TTF and PT at hydrogen bonding sites on PB moieties in the resulting simultaneous CT and PT complexes. iii) The excellent chelating ability of the PB unit should provide opportunities for the complexation of a wide range of transition metals to the donor system giving rise to diverse structural chemistry and appealing photophysics. The results reported here are part of an initial exploratory study of their potential to generate a range of well-defined coordination networks as well as to produce the simultaneous CT and PT complexes. Currently, we are engaged in an investigation on the ability to bind transition metal ions and to form CT complexes and ion radical salts of these promising new donors.

Experimental Section

General

Melting points were determined using a Büchi 510 instrument and are uncorrected. Elemental analyses were performed on a Carlo Erba Instruments EA 1110 Elemental Analyzer CHN. ^1H and ^{13}C NMR spectra were

obtained using a Bruker AC 300 spectrometer operating at 300.18 and 75.5 MHz, respectively: chemical shifts are reported in ppm referenced to residual solvent protons ([D_6]DMSO). The following abbreviations were used: s (singlet), d (doublet), t (triplet), br (broad), and m (multiplet). Infrared spectra were recorded on a Perkin–Elmer Spectrum One FT-IR spectrometer using KBr pellets. EI Mass spectra were recorded using an Auto SpecQ spectrometer. Cyclic voltammetry was conducted on a VA-Stand 663 electrochemical analyzer. An Ag/AgCl electrode containing 2 M LiCl (in ethanol) served as reference electrode, a glassy carbon electrode as counter electrode, and a Pt wire as working electrode. Cyclic voltammetric measurements were performed at room temperature under N_2 in CH_2Cl_2 with 0.1 M Bu_4NPF_6 as supporting electrolyte at a scan rate of 100 mV s^{-1}.

Photophysical Measurements

Photophysical measurements were performed on solutions of the compounds **1–3** and the reference compound **PB** in CH_2Cl_2 at room temperature. Unless otherwise stated, the concentration was 10^{-5} M. Absorption spectra were recorded on a Varian Cary 5000 UV/Vis/NIR spectrophotometer. Photometric titrations were performed by recording full absorption spectra as a function of equivalents of HCl added to dissolve in diethyl ether (10^{-2} M). Dilution effects were taken into account in evaluating the spectra. Data analysis was performed using the commercial software SPECFIT/32[29] in order to identify the number of species by factor analysis and to follow the evolution of the species as a function of HCl added by single value decomposition[28] on the basis of the acid–base equilibria of Scheme 2. The least-squares fitting procedure yields the two pK_a values and the spectra of the individual species.

Materials

Unless otherwise stated, all reagents were purchased from commercial sources and used without additional purification. 5,6-Diamino-2-(4,5-bis-(propylthio)-1,3-dithio-2-ylidene)-benzo[*d*]-1,3-dithiole was prepared according to literature procedures.[10–11]

Synthesis

1: Pyridinecarboxaldehyde (0.1 mL, 1 mmol) was added to a solution of 5,6-diamino-2-(4,5-bis(propylthio)-1,3-dithio-2-ylidene)-benzo[*d*]-1,3-dithiole (0.43 g, 1 mmol) in cold 1,4-dioxane (50 mL). The mixture was open to air and stirred for 24 h. The solvent was evaporated in vacuum and the resulting crude product was purified by chromatography on silica gel with CH_2Cl_2/ethylacetate (2:1) to obtain **1** (0.145 g, 0.28 mmol, 28%) as a light-orange solid. M.p.: 145–147 °C; ^{1}H NMR: δ = 0.96 (t, 6H), 1.59 (m, 4H), 2.86 (t, 4H), 7.53 (m, 1H), 7.66 (s, 1H), 7.88 (s, 1H), 8.00 (m, 1H), 8.29 (m, 1H), 8.73 (m, 1H), 13.24 ppm (s, 1H); ^{13}C NMR: δ = 12.69, 22.58, 37.36, 79.11, 108.31, 112.65, 121.45, 124.84, 126.86, 137.54, 147.94, 149.39, 151.66 ppm; IR (KBr) $\tilde{\nu}$ = 3431, 2959, 1627, 1596, 1444, 1392, 1088, 882, 791 cm^{-1}; MS(EI): *m*/*z* (%): 519 (45) [M^+]; elemental analysis: calcd (%) for $C_{22}H_{21}N_3S_6$: C 50.83, H 4.07, N 8.08; found: C 51.12, H 4.16, N 7.42. Single crystals were obtained by slowly cooling a hot acetonitrile solution of **1**.

General procedure for 2–3: A solution of the corresponding aldehyde (0.1 mmol) and 5,6-diamino-2-(4,5-bis(propylthio)-1,3-dithio-2-ylidene)-benzo[*d*]-1,3-dithiole (0.04 g, 0.1 mmol) in nitrobenzene (10 mL) was heated up to 160 °C for 20 h. The solvent was evaporated in vacuum and the resulting crude product was purified by chromatography on silica gel with CH_2Cl_2/ethylacetate (2:1) to obtain an analytically pure product.

2: Yield: 0.02 g (40%), orange solid. M.p.: 208–210 °C; ^{1}H NMR: δ = 0.96 (t, 6H), 1.59 (m, 4H), 2.86 (t, 4H), 7.68 (m, 1H), 7.73 (s, 1H), 7.86 (m, 1H), 7.94 (s, 1H), 8.05 (m, 1H), 8.13 (m, 1H), 8.40 (d, 1H), 8.53 (d, 1H), 13.34 ppm (s, 1H); ^{13}C NMR: δ = 12.72, 22.63, 37.40, 106.03, 108.51, 112.60, 113.11, 119.13, 126.85, 126.92, 127.37, 128.08, 128.21, 128.69, 129.40, 130.50, 130.95, 134.48, 137.43, 143.35, 147.16, 148.16, 151.63 ppm; IR (KBr) $\tilde{\nu}$ = 3431, 2959, 1611, 1538, 1450, 1314, 1084, 852 cm^{-1}; MS(EI): *m*/*z* (%): 569 (40) [M^+]; elemental analysis: calcd (%) for $C_{26}H_{23}N_3S_6$: C 54.80, H 4.07, N 7.37; found: C 54.99, H 4.12, N 6.83.

3: Yield: 0.02 g (38%), yellow solid. M.p.: 235–237 °C; ^{1}H NMR: δ = 0.96 (t, 6H), 1.60 (m, 4H), 2.86 (t, 4H), 3.94 (s, 3H) 7.47 (m, 2H), 7.80 (s, 2H), 8.03 (d, 1H), 8.37 (m, 2H), 12.68 ppm (b, 1H); ^{13}C NMR: δ = 12.72, 22.61, 37.39, 55.65, 106.06, 108.34, 112.72, 119.43, 122.94, 126.88, 129.40, 129.74, 130.19, 136.03, 143.13, 145.83, 152.00, 157.95 ppm; IR (KBr) $\tilde{\nu}$ = 3435, 2961, 1622, 1611, 1600, 1504, 1394, 1377, 1241, 833 cm^{-1}; MS(EI): *m*/*z* (%): 599 (40) [M^+]; elemental analysis: calcd (%) for $C_{27}H_{25}N_3OS_6$: C 54.06, H 4.02, N 7.00; found: C 54.33, H 4.24, N 6.67.

Crystallography

An orange crystal of compound **1** was mounted on a Stoe Mark II-Imaging Plate Diffractometer System (Stoe & Cie, 2002) equipped with a graphite-monochromator. Data collection was performed at −100 °C using $Mo_{K\alpha}$ radiation (λ = 0.71073 Å). 245 exposures (4 min per exposure) were obtained at an image plate distance of 100 mm, 180 frames with ϕ = 0° and 0° < ω < 180°, and 65 frames with ϕ = 90° and 0° < ω < 97°, with the crystal oscillating through 1° in ω. The resolution was: D_{min}–D_{max} = 0.72–17.78 Å. The structure was solved by direct methods using the program SHELXS-97[30] and refined by full matrix least squares on F^2 with SHELXL-97.[31] The NH hydrogen atom was derived from Fourier difference maps and refined while the remaining hydrogen atoms were included in calculated positions and treated as riding atoms using SHELXL-97 default parameters. All non-hydrogen atoms were refined anisotropically. No absorption correction was applied.

Crystal data for **1**: $C_{22}H_{21}N_3S_6$, M = 519.78, 0.45 × 0.20 × 0.15 mm^3, monoclinic, space group *C*2/*c*, *a* = 40.925(3), *b* = 7.4182(4), *c* = 15.3202(11) Å, β = 100.778(6)°, *V* = 4569.0(6) $Å^3$, *Z* = 8, ρ_{calcd} = 1.511 g cm^{-3}, μ = 0.616 mm^{-1}, *T* = 173(2) K, *F*(000) = 2160, 29100 reflections collected, 6183 unique (R_{int} = 0.0891). Final GOF = 1.029, R_1 = 0.0564, wR_2 = 0.1465, *R* indices based on 4693 reflections with $I > 2\sigma(I)$, 287 parameters, 0 restraints. CCDC 699063 contains the supplementary crystallographic data for **1**. These data can be obtained free of charge from The Cambridge Crystallographic Data Centre at www.ccdc.cam.ac.uk/data_request/cif

Acknowledgements

This work was supported by the Swiss National Science Foundation (grant No. 200020-116003 and 200020-115867).

[1] a) R. L. Carroll, C. B. Gorman, *Angew. Chem.* **2002**, *114*, 4556–4579; *Angew. Chem. Int. Ed.* **2002**, *41*, 4378–4400; b) E. Tsiperman, J. Y. Becker, V. Khodorkovsky, A. Shames, L. Shapiro, *Angew. Chem.* **2005**, *117*, 4083–4086; *Angew. Chem. Int. Ed.* **2005**, *44*, 4015–4018.

[2] a) *TTF Chemistry: Fundamentals and Applications of Tetrathiafulvalene* (Eds.: J.-I. Yamada, T. Sugimoto), Springer, Berlin, Germany, **2004**; b) V. Khodorkovsky, J. Y. Becker, *Organic Conductors: Fundamentals and Applications* (Ed.: J. P. Farges), Marcel Dekker, New York, NY, **1994**, chap. 3; c) J. M. William, J. R. Ferraro, R. J. Thorn, K. D. Carlson, U. Geiser, H. H. Wang, A. M. Kini, M. H. Whangbo, *Organic Superconductors (Including Fullerenes): Synthesis Structure, Properties, and Theory*, Prentice Hall, Englewoods Cliffs, NJ, **1992**; d) G. Saito, Y. Yoshida, *Bull. Chem. Soc. Jpn.* **2007**, *80*, 1–137.

[3] H. M. Yamamoto, R. Kato, *Chem. Lett.* **2000**, 970–971.

[4] a) S.-X. Liu, A. Neels, H. Stoeckli-Evans, M. Pilkington, J. D. Wallis, S. Decurtins, *Polyhedron* **2004**, *23*, 1185–1189; b) M. Fourmigué, P. Batail, *Chem. Rev.* **2004**, *104*, 5379–5418; c) S. A. Baudron, P. Batail, C. Coulon, R. Clérac, E. Canadell, V. Laukhin, R. Melzi, P. Wzietek, D. Jérome, P. Auban-Senzier, S. Ravy, *J. Am. Chem. Soc.* **2005**, *127*, 11785–11797; d) Y. Morita, S. Maki, M. Ohmoto, H. Kitagawa, T. Okubo, T. Mitani, K. Nakasuji, *Org. Lett.* **2002**, *4*, 2185–2188; e) P. Blanchard, K. Boubekeur, M. Sallé, G. Duguay, M. Jubault, A. Gorgues, J. D. Martin, E. Canadell, P. Auban-Senzier, D. Jérome, P. Batail, *Adv. Mater.* **1992**, *4*, 579–581; f) E. Miyazaki, Y. Morita, Y. Yakiyama, S. Maki, Y. Umemoto, M. Ohmoto, K. Nakasuji, *Chem. Lett.* **2007**, *36*, 1102–1103; g) Y. Morita, E. Miyazaki, Y. Umemoto, K. Fukui, K. Nakasuji, *J. Org. Chem.* **2006**, *71*, 5631–5637.

[5] a) T. Murata, Y. Morita, Y. Yakiyama, K. Fukui, H. Yamochi, G. Saito, K. Nakasuji, *J. Am. Chem. Soc.* **2007**, *129*, 10837–10846; b) T. Murata, Y. Morita, K. Fukui, K. Sato, D. Shiomi, T. Takui, M. Maesato, H. Yamochi, G. Saito, K. Nakasuji, *Angew. Chem.* **2004**, *116*, 6503–6506; *Angew. Chem. Int. Ed.* **2004**, *43*, 6343–6346; c) Y. Morita, Y. Yamamoto, Y. Yakiyama, T. Murata, K. Nakasuji, *Chem. Lett.* **2008**, *37*, 24–25; d) T. Murata, Y. Morita, Y. Yakiyama, Y. Nishimura, T. Ise, D. Shiomi, K. Sato, T. Takuic, K. Nakasuji, *Chem. Commun.* **2007**, 4009–4011.

[6] a) G. J. Ashwell, W. D. Tyrrell, A. J. Whittam, *J. Am. Chem. Soc.* **2004**, *126*, 7102–7110; b) G. Ho, J. R. Heath, M. Kondratenko, D. F. Perepichka, K. Arseneault, M. Pézolet, M. R. Bryce, *Chem. Eur. J.* **2005**, *11*, 2914–2922; c) R. M. Metzger, J. W. Baldwin, W. J. Shumate, I. R. Peterson, P. Mani, G. J. Mankey, T. Morris, G. Szulczewski, S. Bosi, M. Prato, A. Comito, Y. Rubin, *J. Phys. Chem. B* **2003**, *107*, 1021–1027; d) R. M. Metzger, *Acc. Chem. Res.* **1999**, *32*, 950–957; e) H. Meier, *Angew. Chem.* **2005**, *117*, 2536–2561; *Angew. Chem. Int. Ed.* **2005**, *44*, 2482–2506; f) D. M. Guldi, F. Giacalone, G. de La Torre, J. L. Segura, N. Martin, *Chem. Eur. J.* **2005**, *11*, 7199–7210; g) F. Giacalone, J. L. Segura, N. Martín, D. M. Guldi, *J. Am. Chem. Soc.* **2004**, *126*, 5340–5341; h) C. Atienza, N. Martín, M. Wielopolski, N. Haworth, T. Clark, D. M. Guldi, *Chem. Commun.* **2006**, 3202–3204; i) M. Wielopolski, C. Atienza, T. Clark, D. M. Guldi, N. Martín, *Chem. Eur. J.* **2008**, *14*, 6379–6390.

[7] N. Gautier, F. Dumur, V. Lloveras, J. Vidal-Gancedo, J. Veciana, C. Rovira, P. Hudhomme, *Angew. Chem.* **2003**, *115*, 2871–2874; *Angew. Chem. Int. Ed.* **2003**, *42*, 2765–2768.

[8] M. Bendikov, F. Wudl, D. F. Perepichka, *Chem. Rev.* **2004**, *104*, 4891–4946.

[9] a) C. Loosli, C. Jia, S.-X. Liu, M. Haas, M. Dias, E. Levillain, A. Neels, G. Labat, A. Hauser, S. Decurtins, *J. Org. Chem.* **2005**, *70*, 4988–4992; b) C. A. Donders, S.-X. Liu, C. Loosli, L. Sanguinet, A. Neels, S. Decurtins, *Tetrahedron* **2006**, *62*, 3543–3549; c) S. Delahaye, C. Loosli, S.-X. Liu, S. Decurtins, G. Labat, A. Neels, A. Loosli, T. R. Ward, A. Hauser, *Adv. Funct. Mater.* **2006**, *16*, 286–295.

[10] C.-Y. Jia, S.-X. Liu, C. Tanner, C. Leiggener, L. Sanguinet, E. Levillain, S. Leutwyler, A. Hauser, S. Decurtins, *Chem. Commun.* **2006**, 1878–1880.

[11] C. Jia, S.-X. Liu, C. Tanner, C. Leiggener, A. Neels, L. Sanguinet, E. Levillain, S. Leutwyler, A. Hauser, S. Decurtins, *Chem. Eur. J.* **2007**, *13*, 3804–3812.

[12] J. C. Wu, S.-X. Liu, T. D. Keene, A. Neels, V. Mereacre, A. K. Powell, S. Decurtins, *Inorg. Chem.* **2008**, *47*, 3452–3459.

[13] C. Goze, C. Leiggener, S.-X. Liu, L. Sanguinet, E. Levillain, A. Hauser, S. Decurtins, *ChemPhysChem* **2007**, *8*, 1504–1512.

[14] a) M. R. Grimmett, *Comprehensive Heterocyclic Chemistry*, *Vol. 3* (Eds.: A. R. Katrizky, C. W. Rees, E. F. V. Scriven), Pergamon, Oxford, **1996**, 77–220; b) P. N. Preston, M. F. G. Stevens, G. Tennant, *Benzimidazoles and Congeneric Tricyclic Compounds*, *Part 2*, Wiley, New York, **1980**; c) G. Navarrete-Vazquez, R. Cedillo, A. Hernandez-Campos, L. Yepez, F. Hernandez-Luis, J. Valdez, R. Morales, R. Cortes, M. Hernandez, R. Castillo, *Bioorg. Med. Chem. Lett.* **2001**, *11*, 187–190.

[15] S. Iwata, C. Ostermeier, B. Ludwig, H. Michel, *Nature* **1995**, *376*, 660–669.

[16] a) L. J. Charbonnière, A. F. Williams, C. Piguet, G. Bernardinelli, E. Rivara-Minten, *Chem. Eur. J.* **1998**, *4*, 485–493; b) L. Zhou, Y. Wang, C. Zhou, C. Wang, Q. Shi, S. Peng, *Cryst. Growth Des.* **2007**, *7*, 300–306; c) Y. Morita, T. Murata, S. Yamada, M. Tadokoro, A. Ichimura, K. Nakasuji, *J. Chem. Soc. Perkin Trans. 1* **2002**, *1*, 2598–2600.

[17] a) D. Luneau, P. Rey, *Mol. Cryst. Liq. Cryst.* **1995**, *273*, 81–87; b) J. R. Ferrer, P. M. Lahti, C. George, G. Antorrena, F. Palacio, *Chem. Mater.* **1999**, *11*, 2205–2210.

[18] a) T. Akutagawa, T. Hasegawa, T. Nakamura, T. Inabe, G. Saito, *Chem. Eur. J.* **2002**, *8*, 4402–4411; b) Y. Morita, T. Murata, K. Fukui, S. Yamada, K. Sato, D. Shiomi, T. Takui, H. Kitagawa, H. Yamochi, G. Saito, K. Nakasuji, *J. Org. Chem.* **2005**, *70*, 2739–2744; c) T. Murata, Y. Morita, K. Nakasuji, *Tetrahedron* **2005**, *61*, 6056–6063; d) T. Akutagawa, G. Saito, M. Kusunoki, K.-I. Sakaguchi, *Bull. Chem. Soc. Jpn.* **1996**, *69*, 2487–2511.

[19] a) Q. Zeng, P. Cai, Z. Li, J. Qin, B. Zh. Tang, *Chem. Commun.* **2008**, 1094–1096; b) A. J. Boydston, P. D. Vu, O. L. Dykhno, V. Chang, A. R. Wyatt, A. S. Stockett, E. T. Ritschdorff, J. B. Shear, C. W. Bielawski, *J. Am. Chem. Soc.* **2008**, *130*, 3143–3156; c) L. De La Durantaye, T. McCormick, X.-Y. Liu, S. Wang, *Dalton Trans.* **2006**, 5675–5682.

[20] a) S.-X. Liu, S. Dolder, P. Franz, A. Neels, H. Stoeckli-Evans, S. Decurtins, *Inorg. Chem.* **2003**, *42*, 4801–4803; b) C. Jia, S.-X. Liu, C. Ambrus, A Neels, G. Labat, S. Decurtins, *Inorg. Chem.* **2006**, *45*, 3152–3154; c) J. Wu, S.-X. Liu, A. Neels, F. Le Derf, M. Sallé, S. Decurtins, *Tetrahedron* **2007**, *63*, 11282–11286.

[21] a) J. S. Casas, A. Castiñeiras, E. García-Martínez, Y. Parajóa, M. L. Pérez-Parallé, A. Sánchez-González, J. Sordo, *Z. Anorg. Allg. Chem.* **2005**, *631*, 2258–2264; b) S.-M. Yue, Zh.-M. Su, J.-F. Ma, Y. Liao, Y.-H. Kan, H.-J. Zhang, *Jiegou Huaxue* **2003**, *22*, 174–178.

[22] Cyclic voltammograms of compounds **2** and **3** in the presence of increasing amounts of HCl, are given in Figures S1 and S2 of the Supporting Information.

[23] In the presence of a large excess of HCl (300 equiv), after half an hour the two reversible redox waves were only observed during the potential scans with a freshly polished electrode, and also a concomitant color change occurred. Subsequent multiple cycling of the electrode potential within the measured window and neutralization did not reveal any redox features, indicative of the occurrence of adsorption and decomposition of the TTF compound under strong acidic conditions.

[24] a) Q. Y. Zhu, Y. Liu, W. Lu, Y. Zhang, G. Q. Bian, G. Y. Niu, J. Dai, *Inorg. Chem.* **2007**, *46*, 10065–10070; b) H.-H. Lin, Z.-M. Yan, J. Dai, D.-Q. Zhang, J.-L. Zuo, Q.-Y. Zhu, D.-X. Jia, *New J. Chem.* **2005**, *29*, 509–513.

[25] a) T. Abbaz, A.-K. Gouasmia, H. Fujiwara, T. Hiraoka, T. Sugimoto, M. Taillefer, J.-M. Fabre, *Synth. Met.* **2007**, *157*, 508–516; b) H. J. Hartigan, G. Seeber, A. R. Mount, L. J. Yellowlees, N. Robertson, *New J. Chem.* **2004**, *28*, 98–103; c) M. Mosimann, S.-X. Liu, G. Labat, A. Neels, S. Decurtins, *Inorg. Chim. Acta* **2007**, *360*, 3848–3854; d) C. Jia, D. Zhang, Y. Xu, W. Xu, H. Hu, D. Zhu, *Synth. Met.* **2003**, *132*, 249–255; e) S. Bouguessa, K. Hervé, S. Golhen, L. Ouahab, J.-M. Fabre, *New J. Chem.* **2003**, *27*, 560–564.

[26] C. J. Chang, C. H. Yang, K. Chen, Y. Chi, C. F. Shu, M. L. Ho, Y. S. Yeh, P. T. Chou, *Dalton Trans.* **2007**, 1881–1890.

[27] a) J. Smets, W. McCarthy, G. Maes, L. Adamowicz, *J. Mol. Struct.* **1999**, *476*, 27–43; b) M. Novo, M. Mosquera, F. R. Prieto, *Can. J. Chem.* **1992**, *70*, 823–827.

[28] G. Puxty, M. Maeder, K. Hungerbühler, *Chemom. Intell. Lab. Syst.* **2006**, *81*, 149–164.

[29] SPECFIT/32, Spectrum Software Associates, Marlborough, MA, **2005**.

[30] G. M. Sheldrick, *Acta Crystallogr. Sect. A* **2008**, *64*, 112–122.

[31] G. M. Sheldrick, *SHELXL-97*, *Program for Crystal Structure Refinement*, University of Göttingen, Göttingen, Germany, **1997**.

Received: August 21, 2008
Published online: December 29, 2008

